Li$_2$NaV$_2$(PO$_4$)$_3$: A 3.7 V Lithium-Insertion Cathode with the Rhombohedral NASICON Structure

Brian L. Cushing and John B. Goodenough[1]

Texas Materials Institute, Mail Code C2201, The University of Texas at Austin, Austin, Texas 78712

Li$_2$NaV$_2$(PO$_4$)$_3$ **has been prepared in the rhombohedral NASI-CON structure via ion exchange from** Na$_3$V$_2$(PO$_4$)$_3$. **As a lithium-insertion cathode material,** Li$_2$NaV$_2$(PO$_4$)$_3$ **exhibits a specific discharge capacity of** $\sim$96 mAh g^{-1} **at a current density of 0.50 mA cm^{-2} with a clear plateau near 3.7 V versus lithium metal. Approximately 10% of the capacity is lost through the first 50 cycles, after which the capacity appears to stabilize. During charge and discharge, the Na$^+$ ions tend to remain immobilized in the $A(1)$ site of the NASICON structure, suggesting a direct $A(2) \to A(2)$ lithium-transport mechanism.**

© 2001 Elsevier Science

Key Words: lithium-insertion compounds; battery; lithium-ion; ion-exchange; mixed alkali–ion conduction.

INTRODUCTION

NASICON (for Na$^+$ superionic conductor)-related compounds have been shown to be promising cathode materials for lithium-ion batteries, exhibiting high Li$^+$ mobility and reasonable discharge capacities (1–6). Table 1 details the relevant characteristics of several NASICON-related cathode materials. From Table 1, the transition metals with the most useful redox potentials are Fe^{2+}/Fe^{3+} in a sulfate framework and V^{3+}/V^{4+} in a phosphate framework. Fe$_2$(SO$_4$)$_3$ has already been thoroughly investigated as a cathode material for lithium-ion batteries (2, 3). Here, we report our investigation of the NASICON-related rhombohedral Li$_2$NaV$_2$(PO$_4$)$_3$ as a high-voltage cathode material.

Cursory examination of the NASICON structure reveals its potential as a lithium-insertion cathode. NASICON-related compounds with the highest ionic mobilities possess rhombohedral ($R\bar{3}$) symmetry (7). The $M_2(XO_4)_3$ framework is built of $(XO_4)^{n-}$ ($X = $ Si^{4+}, P^{5+}, S^{6+}, Mo^{6+}, etc.) tetrahedra corner-linked to octahedral-site M^{m+} ($M = $ transition metal) (8). The alkali ions can occupy two different sites. At low alkali content (i.e., $x \leq 1$ in $A_xM_2(XO_4)_3$),

an octahedral site, $A(1)$, is selectively occupied (Fig. 1) (8). With $x > 1$, the alkali ions are randomly distributed among the $A(1)$ and three 8-coordinate sites, $A(2)$. The open, 3D nature of the structure allows easy migration of the alkali ions between $A(1)$ and $A(2)$, and the exceptional ionic mobility of the alkali ions is well documented (7).

A NASICON phase, Li$_3$V$_2$(PO$_4$)$_3$, has been previously investigated as a cathode material in lithium batteries (9,10). Like many NASICON-related compounds, however, Li$_3$V$_2$(PO$_4$)$_3$ prepared by direct reaction is not rhombohedral. The Li$_3$V$_2$(PO$_4$)$_3$ phases previously investigated assume the monoclinic ($P2_1/n$) and orthorhombic NASICON structures. The compounds give discharge capacities approaching 131 mAh g^{-1}, but they also exhibit multiple plateaus in their discharge curves (at 4.1, 3.7, and 3.6 V). Furthermore, previous studies have demonstrated that the monoclinic NASICON modification exhibits reduced alkali-ion mobility relative to the rhombohedral form (6, 7). While Li$_3$V$_2$(PO$_4$)$_3$ apparently cannot be prepared in the rhombohedral NASICON structure by direct reaction, rhombohedral Na$_3$V$_2$(PO$_4$)$_3$ has been reported (11) and thus provides a suitable starting material for a topotactic ion exchange of Li$^+$ for Na$^+$.

EXPERIMENTAL

Li$_2$NaV$_2$(PO$_4$)$_3$ was prepared via ion exchange from Na$_3$V$_2$(PO$_4$)$_3$. Na$_3$V$_2$(PO$_4$)$_3$ was prepared by direct reaction of NaPO$_3$ (prepared by dehydration of NaH$_2$PO$_4$ (GFS, 99%)) and V$_2$O$_3$ (Aldrich, 99%) in a 3:1 molar ratio. The reactants were ground under acetone with an agate mortar and pestle. After drying, the mixture was placed in an alumina boat and heated at 1°C min^{-1} to 900°C under a 10% H$_2$/Ar mixture flowing at $\sim$25 mL min^{-1}. The sample was held at 900°C for 2 days and slowly cooled to room temperature by turning off the furnace. The product was ground under 5% H$_2$SO$_4$ to remove any unreacted phosphates, collected by vacuum filtration, and dried at 150°C in air.

TABLE 1
Lithium-Insertion Properties of Selected NASICON-Type Compounds

Compound (Ref.)	Structure type[a]	Redox couple	Redox potential (V)	Number of Li^+ atoms inserted	Reversible discharge capacity (mAh g^{-1})[b] and current (mA cm^{-2})
$Fe_2(SO_4)_3$ (2)	R	Fe^{3+}/Fe^{2+}	3.6	2	134 @ 0.015
	M	Fe^{3+}/Fe^{2+}	3.6	2	134 @ 0.015
$V_2(SO_4)_3$ (4)	R	V^{3+}/V^{2+}	2.6	1.8	130 @ 0.5
$LiTi_2(PO_4)_3$ (5)	R	Ti^{4+}/Ti^{3+}	2.5	2.3	160 @ 0.05
				1.5	110 @ 0.5
				1.2	80 @ 1.0
$Li_{3-x}Fe_2(PO_4)_3$ (2, 6)	M	Fe^{3+}/Fe^{2+}	2.8	1.6	105 @ 0.05
				1.1	75 @ 0.5
				0.75	55 @ 1.0
$Li_{3-x}FeV(PO_4)_3$ (2)	M	V^{4+}/V^{3+}	3.8	1.6	110 @ 0.075
		V^{3+}/V^{2+}	1.75		
		Fe^{3+}/Fe^{2+}	2.8		

[a] R = rhombohedral form (space group $R\overline{3}$ or $R\overline{3}c$); M = monoclinic form (space group $P2_1/n$).

[b] Discharge capacity given by $[(nF)/(3.6M_w)]$, n = no. of Li^+ atoms inserted per formula unit, F = Faraday's constant (96,485 C mol^{-1}), M_w = molecular weight of fully intercalated compound.

Ion exchange of $Na_3V_2(PO_4)_3$ was carried out in an aqueous solution containing a 100% molar excess of $LiNO_3$ (GFS, 99.9%) at $\sim 40°C$. The NASICON phase was stirred in the nitrate solution overnight, collected by vacuum filtration, and washed with deionized water. The process was twice repeated to ensure maximal Li^+ for Na^+ ion exchange.

Powder X-ray diffraction (XRD) studies were performed on a Philips diffractometer equipped with a Cu$K\alpha$ radiation source ($\lambda = 1.5406$ Å). Finely divided silicon powder (Aldrich, 99.999%) was used as an internal standard. Peak locations and intensities were determined with the JADE software program using a least-squares method (12).
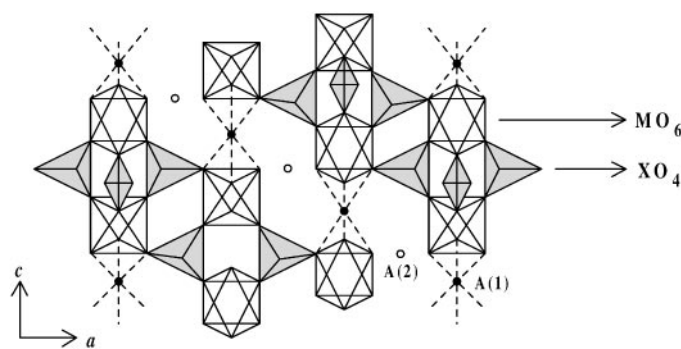

FIG. 1. Idealized representation of the rhombohedral form of the NASICON structure.

Quantitative elemental analysis of lithium was carried out on a Perkin-Elmer 1100 Atomic Absorption Spectrometer (AAS). Samples for AAS were digested in concentrated HNO_3. Quantitative determinations of vanadium were made by potentiometric titrations. Samples for titration were digested in concentrated H_2SO_4. A slight excess of 0.1 M $KMnO_4$ was added to preliminarily oxidize V^{3+} to the pervanadyl ion, VO_2^+. The remaining permanganate was reduced by the addition of sodium nitrite, which was subsequently destroyed by the addition of urea. The VO_2^+ was then potentiometrically titrated with standard ferrous ammonium sulfate solution. The potentiometric equivalence points were determined by the method of Gran (13).

Electrochemical lithium insertion/extraction was investigated by incorporating $Li_2NaV_2(PO_4)_3$ as cathode materials in lithium-ion button cells (type 2320). The NASICON phase was combined in a 70:25:5 proportion with acetylene black to improve conductivity and polytetrafluoroethylene (PTFE) as a binder. The resulting mixture was rolled into a thin sheet from which 1 cm^2 cathode discs of uniform thickness were cut. Cell assembly was carried out in an argon-filled glove box. A 1 M solution of $LiClO_4$ in a 50/50 mixture of propylene carbonate and dimethoxyethane composed the electrolyte. For the button cells, Celgard 2500 served as the separator. The cells were cycled between 2.5 and 4.1 V at 0.50, 1.0, and 2.0 mA cm^{-2} against a lithium metal anode on an Arbin BT2043 Battery Test System.

Chemical sodium extraction from $Na_3V_2(PO_4)_3$ was performed by oxidative deintercalation. The NASICON phase was suspended in acetonitrile under inert atmosphere and a 100% molar excess of 1 M NO_2PF_6 in acetonitrile was added with standard Schlenk techniques. The mixture was stirred at room temperature for two days under an inert atmosphere. The product was collected by vacuum filtration, washed with acetonitrile, and dried under vacuum.

RESULTS AND DISCUSSION

$Li_2NaV_2(PO_4)_3$ was obtained via ion exchange of the sodium analogue. Consistent with the findings of others (14), $Na_3V_2(PO_4)_3$ decomposed in molten $LiNO_3$, necessitating that the ion exchange take place in solution at relatively low temperature. During the exchange process, a faint blue coloration of the solution was observed, indicating partial dissolution of the sample. At temperatures above 40°C, the sample dissolution became excessive. Quantitative elemental analysis revealed a final composition of $Li_{1.98}Na_{1.02}V_2(PO_4)_3$, referred to here as $Li_2NaV_2(PO_4)_3$ (Table 2).

Whereas Gopalakrishnan and Kasthuri Rangan (15) reported complete extraction of Na^+, we could not oxidatively extract all the Na^+ from $Na_3V_2(PO_4)_3$; the composition of our deintercalated product was $Na_{0.99}V_2(PO_4)_3$. This may reflect differences in the experi-

TABLE 2
Elemental Analysis Results for $A_xV_2(PO_4)_3$

Compound	% Li [expected]	% Na [expected]	% V [expected]	Experimental composition
$Na_3V_2(PO_4)_3$ (starting material)	—	15.15(4) [15.13]	22.34(5) [22.35]	$Na_{3.00}V_{2.00}(PO_4)_3$
$Li_2NaV_2(PO_4)_3$ (Exchange product)	3.24(2) [3.28]	5.53(3) [5.43]	24.03(4) [24.05]	$Li_{1.98}Na_{1.02}V_{2.00}(PO_4)_3$
$NaV_2(PO_4)_3$ (Deintercalation product)	—	5.56(2) [5.61]	24.88(3) [24.86]	$Na_{0.99}V_{2.00}(PO_4)_3$

mental methods, as we used NO_2PF_6 as an oxidizing agent as opposed to chlorine gas.

The XRD results for $Li_2NaV_2(PO_4)_3$ indicate that $Li_2NaV_2(PO_4)_3$ retains the rhombohedral NASICON structure of its precursor (Tables 3, 4; Fig. 2). The XRD results reveal a substantial contraction of the a parameter and expansion of the c parameter of the rhombohedral NASICON unit cell as Na^+ is replaced by Li^+. This is consistent with the behavior of other NASICON compounds such as $Na_3Fe_2(PO_4)_3$ during Li^+ for Na^+ ion exchange (6, 16). Those authors attributed the changes to a redistribution of the alkali ions away from $A(1)$ such that some or all of the $A(1)$ sites are left vacant, which introduces a strong electrostatic repulsion along the c axis across the $A(1)$ site. Delmas *et al.* have demonstrated with neutron diffraction experiments that the exceptional lithium ion conductivity of $Li_{1+x}Ti_2(PO_4)_3$ is due in part to the tendency of Li^+ to migrate out of $A(1)$ to $A(2)$ (5). Thus, it would appear that the Li^+ cation has a preference for the $A(2)$ site. There is no evidence, however, to indicate a similar behavior for Na^+, and in the case of $Li_2NaV_2(PO_4)_3$, Na^+ may selectively occupy $A(1)$; otherwise, the Na^+ ion should have exchanged for Li^+ during the ion-exchange process. Li^+ is

too small to coordinate at the center of a large, eight-coordinate cavity like $A(2)$; if Li^+ is displaced from the center of the cavity, the electrostatic attraction between Li^+ and O^{2-} could easily account for the changes in the c/a ratio.

Cathode performance. The initial charging of the electrochemical cells results in the oxidation of V^{3+} to V^{4+} as 1.8 lithium atoms per formula unit are extracted at ~ 3.9 V versus lithium. The subsequent discharge produced a single, flat discharge plateau at 3.7 V (Fig. 3). This value is to be compared with 3.8 V for the V^{3+}/V^{4+} couple found for $Li_{3-x}FeV(PO_4)_3$ (see Table 1). Replacement of one Li^+ ion by Na^+ has little influence on the energy of the V^{3+}/V^{4+} couple; the dominant influence is the acidity of the polyanion (1–3). At a current density of 0.50 mA cm^{-2}, the initial discharge capacity was 96 mAh g^{-1}, corresponding to the insertion of 1.5 lithium atoms per formula unit. Consistent with the performance of other NASICON-structured cathodes listed in Table 1, the discharge capacity was diminished by increasing the current density (Fig. 4); the capacity, however, recovered when the current was lowered back to 0.50 mA cm^{-2}. This is indicative of a kinetically slow Li^+ diffusion process arising from the poor electronic conductivity of the NASICON cathode material. Regardless of
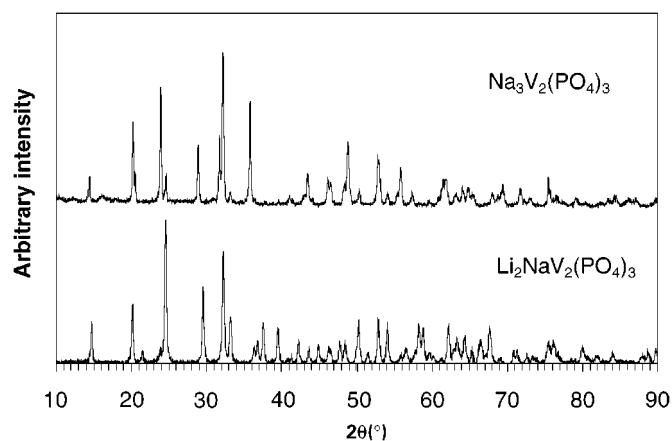

FIG. 2. XRD patterns of $Na_3V_2(PO_4)_3$ and $Li_2NaV_2(PO_4)_3$.

TABLE 3
Summary of Calculated Unit Cells for $A_xV_2(PO_4)_3$

Composition	Calculated unit cell	Literature unit cell
$Na_3V_2(PO_4)_3$	[Hexagonal] $a = 8.642(9)$ Å $c = 21.72(3)$ $V = 1405(5)$ Å^3	[Hexagonal] (11) $a = 8.67(2)$ Å $c = 21.71(3)$ $V = 1413(9)$ Å^3
$Li_2NaV_2(PO_4)_3$	[Hexagonal] $a = 8.325(2)$ $c = 22.491(6)$ $V = 1350(2)$	This work

TABLE 4
XRD Results and Indexing for Li$_2$NaV$_2$(PO$_4$)$_3$

h	k	l			d_{obs} (Å)	d_{calc} (Å)	I/I_o
1	0	2			6.0758	6.0695	15
1	0	4			4.4457	4.4338	32
1	1	0			4.1611	4.1625	12
0	0	6			3.7492	3.7485	17
1	1	3			3.6440	3.6392	100
2	0	4			3.0350	3.0347	48
1	1	6			2.7866	2.7855	77
2	1	1			2.7077	2.7052	33
2	1	4			2.4519	2.4522	14
2	0	7			2.3998	2.3986	27
3	0	3			2.2867	2.2885	25
1	1	9			2.1437	2.1425	14
2	1	7			2.0788	2.0782	4
2	2	1			2.0721	2.0724	4
3	0	6			2.0232	2.0232	15
2	1	8			1.9563	1.9570	8
1	0	10			1.9073	1.9082	6
3	1	4			1.8822	1.8840	12
3	0	8			1.8253	1.8268	9
2	2	6			1.8177	1.8196	22
4	0	2			1.7809	1.7797	4
2	1	10			1.7337	1.7346	33
3	1	7			1.6968	1.6977	23
3	2	1			1.6472	1.6496	2
4	0	6			1.6241	1.6244	6
2	2	9			1.6006	1.5993	8
3	2	4			1.5873	1.5868	1
4	0	7			1.5713	1.5720	17
1	0	14			1.5656	1.5680	2
4	1	3			1.5404	1.5398	5
3	1	10			1.4929	1.4944	25
3	2	7			1.4727	1.4706	1
2	0	14			1.4668	1.4674	26
4	1	6			1.4497	1.4507	19
3	2	8			1.4274	1.4256	5
1	1	15			1.4113	1.4107	6
4	0	10			1.4068	1.4065	14
5	0	4			1.3977	1.3967	< 1
2	1	14			1.3842	1.3839	32
2	2	13			1.3302	1.3304	7
0	0	17			1.3234	1.3230	9
1	1	17			1.2600	1.2608	18
3	3	8			1.2440	1.2442	38
3	1	15,	6	0	1.2000	1.1996	17
5	1	8			1.1766	1.1761	7
3	1	16			1.1508	1.1500	8
4	2	12			1.1008	1.1021	7

current density, capacity fade was evident until about the 50th cycle, at which point the capacities appear to stabilize (Fig. 4).

The presence of Na$^+$ in the cathode material does not lead to cell failure, at least to 100 cycles. Discharge capacity was diminished by about 10% after 50 cycles, but then appeared to stabilize. Previous studies of NASICON cathode materials that contain only Li$^+$ in the A sites, e.g., Li$_3$Fe$_2$(PO$_4$)$_3$, also indicate early capacity fade (2, 6), but to
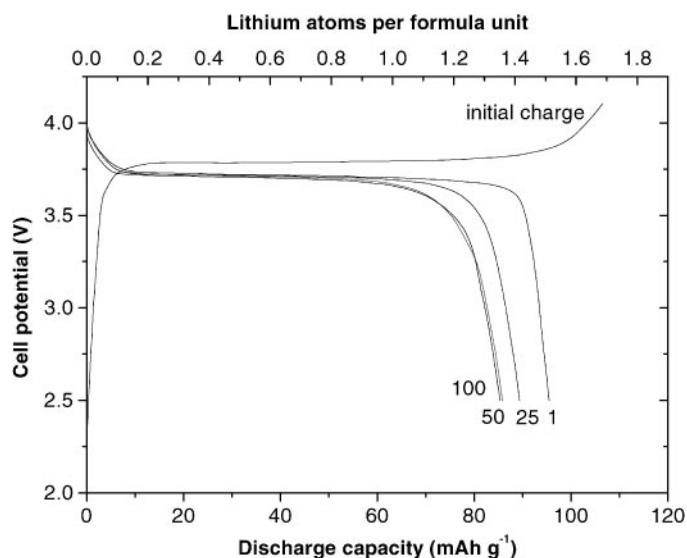

FIG. 3. Electrochemical insertion/extraction of rhombohedral Li$_2$NaV$_2$(PO$_4$)$_3$ at a current density of 0.50 mA cm^{-2}.

our knowledge, the long-term cycle life of these cathode materials has not been investigated.

Ion-transport mechanism. The ion-exchange behavior of Na$_3$V$_2$(PO$_4$)$_3$ suggests that the two Na$^+$ ions in the $A(2)$ sites are mobile, and thus exchange with Li$^+$, while the Na$^+$ in the $A(1)$ site is not. This result is difficult to reconcile with the established ion-transport mechanism of the rhombohedral NASICON structure, which requires a correlated motion involving both $A(1)$ and $A(2)$ sites:
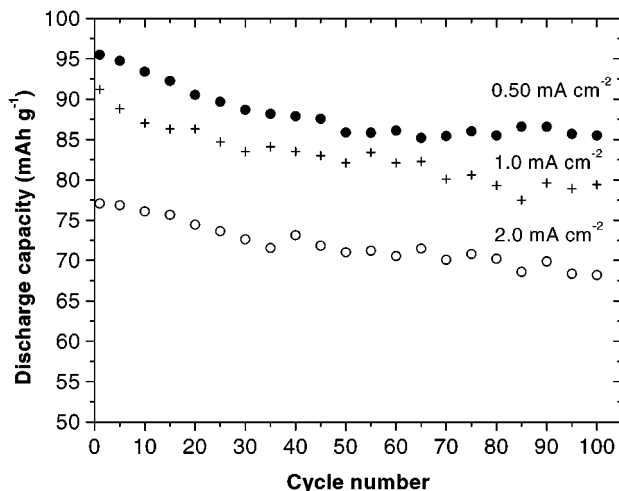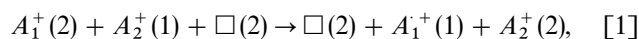
$$A_1^+(2) + A_2^+(1) + \square(2) \to \square(2) + A_1^+(1) + A_2^+(2), \quad [1]$$

FIG. 4. Discharge capacities of rhombohedral Li$_2$NaV$_2$(PO$_4$)$_3$ at various current densities as a function of cycle number.
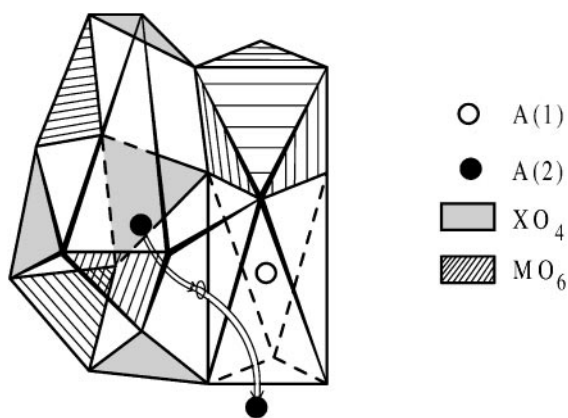
FIG. 5. Ion transport pathway between adjacent $A(2)$ sites in the rhombohedral NASICON structure.

where A represents an alkali ion, the number in parentheses denotes the alkali ion in an $A(1)$ or $A(2)$ site, and $\square$ represents a vacancy (7). Thus, if the Na^+ ions move in a correlated motion between $A(1)$ and $A(2)$, the ions at both sites should be equally capable of being exchanged for Li^+. Likewise, by the mechanism in Eq. [1], both the Na^+ ions situated at $A(1)$ and the Li^+ ions at $A(2)$ of $Li_2NaV_2(PO_4)_3$ should be capable of being extracted from the structure upon electrochemical charging.

To verify whether the Na^+ ions were indeed stationary, the button cells used in the Li^+ insertion/extraction experiments were recharged and opened after completion of their 100th cycle and the Na:V ratio in the cathode materials was determined by quantitative elemental analysis. After 100 cycles, 25% of the Na^+ ions remained in the cathode material. The Na^+ ions that transport out of the NASICON cathode most likely do so while the vanadium is in a mixed III/IV oxidation state, i.e., when $0 < x < 2$ in $Li_xNaV_2(PO_4)_3$. At $x = 0$, only $A(1)$ is occupied and a Na^+ ion in that site tends to be immobilized (7). The $x = 2$ condition was realized during the ion-exchange process, yet the Na^+ in $A(1)$ clearly did not transport. For the bulk of the time during the charge and discharge processes, the NASICON cathode material exists between the $x = 0$ and $x = 2$ end members, when vanadium is present in varying concentrations of V^{3+} and V^{4+}. It seems plausible, then, that the oxidation of vanadium to V^{4+} and the corresponding contraction of its ionic radius introduces a structural distortion to the NASICON framework that reduces the energy difference between $A(1)$ and $A(2)$ and thereby lowers the activation energy of the $A(1) \rightarrow A(2)$ transport pathway.

Notwithstanding the means by which Na^+ eventually escapes $A(1)$, the ion-exchange behavior of $Na_3V_2(PO_4)_3$ and the charge/discharge results of $Li_2NaV_2(PO_4)_3$ strongly suggest that Eq. [1] is not the primary ionic transport pathway of this NASICON compound. One possibility is

that a direct $A(2) \rightarrow A(2)$ motion is occurring:

$$Li^+(2) + Na^+(1) + \square(2) \rightarrow \square(2) + Na^+(1) + Li^+(2). \quad [2]$$
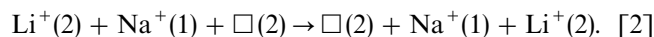
Interestingly, the possibility of a direct $A(2) \rightarrow A(2)$ conduction pathway has been previously postulated by others (17–21). Whether the $A(2) \rightarrow A(2)$ mechanism is the prevalent conduction in any rhombohedral NASICON compound is a point of contention, but based solely on the geometric considerations of Li^+ passing through the opening between adjacent $A(2)$ sites, there is no reason to believe that Eq. [2] is not viable (Fig. 5). Mazza has recently demonstrated with bond-valence calculations that in certain circumstances the $A(2) \rightarrow A(2)$ mechanism can be favored (21). The evidence here suggests that this is precisely the situation in $Li_2NaV_2(PO_4)_3$.

CONCLUSIONS

The low-temperature ion exchange of $Na_3V_2(PO_4)_3$ resulted in a mixed-alkali NASICON compound, $Li_2NaV_2(PO_4)_3$. As a lithium-insertion cathode, $Li_2NaV_2(PO_4)_3$ produces a discharge capacity of $96\ mAh\,g^{-1}$ at $0.50\ mA\,cm^{-2}$. A 10% capacity fade is evident through the first 50 cycles. The Na^+ ions of $Li_2NaV_2(PO_4)_3$ demonstrate a tendency to remain localized in the $A(1)$ site of the rhombohedral NASICON structure. This compound may represent the first empirical evidence of a NASICON compound in which a direct $A(2) \rightarrow A(2)$ conduction path way is favored over the usual $A(1) \rightarrow A(2) \rightarrow A(1)$ mechanism.

REFERENCES

1. A. Manthiram and J. B. Goodenough, *J. Power Sources* **26,** 403 (1989).
2. K. S. Nanjundaswamy, A. K. Padhi, J. B. Goodenough, S. Okada, H. Ohtsuka, H. Arai, and J. Yamaki, *Solid State Ionics* **92,** 1 (1996).
3. A. K. Padhi, V. Manivannan, and J. B. Goodenough, *J. Electrochem. Soc.* **145,** 1518 (1998).
4. J. Gaubicher, J. Angenaut, Y. Chabre, T. Le Mercier, and M. Quarton, *Mol. Cryst. Liq. Cryst.* **311,** 45 (1998).
5. C. Delmas, A. Nadiri, and J. L. Soubeyroux, *Solid State Ionics* **28–30,** 419 (1988).
6. C. Masquelier, A. K. Padhi, K. S. Nanjundaswamy, and J. B. Goodenough, *J. Solid State Chem.* **135,** 228 (1998).
7. J. B. Goodenough, H. Y.-P. Hong, and J. A. Kafalas, *Mater. Res. Bull.* **11,** 203 (1976).
8. H. Y.-P. Hong, *Mater. Res. Bull.* **11,** 173 (1976).

9. H. Ohkawa; K. Yoshida, M. Saito, K. Uematsu, K. Toda, and M. Sato, *Chem. Lett.* 1017 (1999).

10. Barker and M. Y. Saidi, U.S. Patent 5, 871, 866 (1999).

11. C. Delmas, R. Olazcuaga, F. Cherkaoui, R. Brochu, and G. Le Flem, *C. R. Acad. Sci. Paris Ser. C* **287,** 169 (1978).

12. JADE, Materials Data Inc., Livermore, CA (2000).

13. G. Gran, *Analyst* **77,** 661 (1952).

14. A. K. Padhi, "Mapping Redox Energies of Electrode Materials for Lithium Batteries," Ph.D. Dissertation. University of Texas at Austin, Austin, Texas, 1997.

15. J. Gopalakrishnan and K. Kasthuri Rangan, *Chem. Mater.* **4,** 745 (1992).

16. C. Masquelier, C. Wurm, J. Rodríguez-Carvajal, J. Gaubicher, and L. Nazar, *Chem. Mater.* **12,** 525 (2000).

17. E. R. Losilla, M. A. G. Aranda, S. Bruque, M. A. Paris, J. Sanz, and A. R. West, *Chem. Mater.* **10,** 665 (1998).

18. D. Tran Qui, J. J. Capponi, M. Gondrand, M. Saïb, J. C. Joubert, and R. D. Shannon, *Solid State Ionics* **3/4,** 219 (1981).

19. M. A. Subramanian, P. R. Rudolf, and A. Clearfield, *J. Solid State Chem.* **60,** 172 (1985).

20. F. Cherkaoui, G. Villeneuve, C. Delmas, and P. Hagenmuller, *J. Solid State Chem.* **65,** 293 (1986).

21. D. Mazza, *J. Solid State Chem.* **156,** 154 (2001).